Materials Transactions, Vol. 53, No. 3 (2012) pp. 508 to 512

Formation of Amorphous TiO_2 Film on Ti Using Anodizing in Concentrated H_3PO_4 Aqueous Solution and Its Osteoconductivity

Dai Yamamoto[1,*], Takanori Iida[1,*], Kensuke Kuroda[1], Ryoichi Ichino[2], Masazumi Okido[1] and Azusa Seki[3]

[1]*Department of Materials Science & Engineering, Graduate School of Engineering, Nagoya University, Nagoya 464-8603, Japan*
[2]*EcoTopia Science Institute, Nagoya University, Nagoya 464-8603, Japan*
[3]*Hamri Co., Ltd., Tokyo 110-0005, Japan*

Anodizing of Ti specimens were performed in concentrated H_3PO_4 aqueous solutions with a purpose to incorporate a large amount of phosphate ion into anodized coatings, and their osteoconductivity was evaluated in *in vivo* test. Ti specimens were anodized in 0.1–11 M H_3PO_4 aqueous solutions up to 200 V at a rate of 0.1 V s^{-1}. Anodized coatings were evaluated with SEM, TEM, XRD, XPS, and laser microscope. Anodized specimens were implanted in rats' tibia for 14 d, and then extracted.

When anodized in concentrated ($\geq$2 M) H_3PO_4 aqueous solutions under spark discharge, crystallized anatase transformed to amorphous anatase by containing a large amount of PO_4^{3-} in crystal lattice of TiO_2. The amorphous anatase coatings had better osteoconductivity than the crystallized anatase coatings. It is not exactly clear what was the intrinsic factor for the high osteoconductivity, but the crystallinity of anatase and/or PO_4^{3-} in the film is considered to be responsible for the difference in bone-forming ability of TiO_2 films.
[doi:10.2320/matertrans.M2011234]

(Received August 1, 2011; Accepted November 25, 2011; Published February 25, 2012)

Keywords: *titanium, anodizing, phosphoric acid, titanium dioxide, amorphous, osteoconductivity*

1. Introduction

Titanium is widely used in dental and orthopedic implants because of its good biocompatibility and high corrosion resistance. The long-term success rates of Ti implants have been well documented by some reseachers.[1,2] However, many failures occur when the bone is of poor quality.[3,4] Various methods have been assessed to improve the clinical performance of Ti implants in poor-quality bone and to shorten the healing period. For example, hydroxyapatite (HAp), which is the main inorganic component of natural bone, is usually used in the form of a coating on a metallic substrate to compensate for its poor intrinsic mechanical properties. In our previous studies, HAp with various surface morphologies,[5–9] carbonate apatite (CO_3Ap), CO_3Ap/Ca-CO_3 composite films,[10] HAp/collagen, and HAp/gelatin composite films[11] were fabricated on Ti substrates using the thermal substrate method, and we have investigated their osteoconductivity in *in vivo* tests in rats' tibia. These studies have revealed that a specific surface morphology strongly accelerates calcification in the cancellous bone part.

Titanium dioxide is receiving much attention as an osteoconductive substance, similar to HAp. TiO_2 has been shown to exhibit strong physicochemical bonding with living bone.[12] Therefore, optimization of the surface properties of TiO_2 coatings is a key technology in improving the osteoconductivity of implants. There are many types of TiO_2-coating methods for Ti substrates, such as thermal oxidation,[13] chemical methods,[14–16] physical vapor deposition,[17,18] and anodizing.[19–22] Anodizing is a popular hydroprocess used to form TiO_2 coatings because it can give various surface properties on TiO_2 by controlling the oxidizing conditions.[19,21,23,24] Many researchers have formed TiO_2 coatings by anodizing in P-containing aqueous solutions and studied their surface properties because phosphorus, which is one of the important elements composing bone, is contained as phosphate ion in anodized coatings.[23,25] Lee *et al.* reported that higher nucleation ability of bioactive Ca–P compounds was shown on the anodic coating formed in solutions containing phosphate as the concentration of phosphoric acid was increased below 0.9 M.[25] In our previous studies, the TiO_2 coating formed by anodizing in 0.1 M H_3PO_4 aqueous solution induced a high level of bone formation on the substrates in *in vivo* testing.[26] We hypothesized that more phosphate ion could be incorporated when much more highly concentrated H_3PO_4 aqueous solutions were used for the electrolyte, and much more bone could be formed on the coatings. However, to our knowledge, TiO_2 coatings anodized in concentrated H_3PO_4 aqueous solutions above 3 M have not been reported. In this study, Ti specimens were anodized in concentrated H_3PO_4 aqueous solutions with a purpose to incorporate a large amount of phosphate ion into anodized coatings, and their osteoconductivity was evaluated in *in vivo* test.

2. Materials and Methods

2.1 Preparation of the Ti substrates

Cp–Ti plates (for evaluating the coatings, area = 1.13 cm^2) and rods (for *in vivo* testing, dimensions = ϕ2 mm × 5 mm) were used as the substrates, and were covered with epoxy resin, except for the face that would be in contact with the aqueous solution. The substrates were polished with emery paper followed by buffing using Al_2O_3 particles (particle size = 0.05 μm). Then, the substrates were cleaned and then degreased with ethanol.

*Graduate Student, Nagoya University

2.2 Anodizing in aqueous solutions

Ti substrates were used as the working electrode, and a Pt coil was used as the counter electrode. The aqueous solution was stirred while anodizing and was kept at a constant temperature (298 K) in a water bath. Aqueous 0.1–11 M H_3PO_4 solutions were used as electrolytic baths. The anodizing potential was increased up to 200 V at a rate of 0.1 V s^{-1}. After reaching a potential of 200 V, the applied voltage was quickly stopped and the specimen was cleaned with distilled water and dried in air.

2.3 Analysis of the coatings

All of the specimens were sterilized using an autoclave unit at 394 K for a period of 20 min before analysis. The surface morphology and cross-sectional image of the substrates were observed using a scanning electron microscope (SEM) and a transmission electron microscope (TEM). The coated films were identified using thin-film X-ray diffraction (XRD), electron beam diffraction (ED), and X-ray photoelectron spectroscopy (XPS). The surface roughness measurements were conducted using a confocal laser scanning microscope with a measurement area of 150 μm × 112 μm. The arithmetical means of the surface roughness (Ra) was used, because this value was not distorted by any local scarring of the specimen.

2.4 *In vivo* tests

Because the experimental procedure for our *in vivo* study was almost the same as described in previous reports,[9] it is described only briefly here. Before surgery, all of the implants were cleaned in distilled water and immersed in a chlorhexidine gluconate solution. Ten-week-old male Sprague Dawley rats (Charles River Japan, Inc., Japan) were used in our experimental procedures. The specimens were implanted in the tibial metaphysis of the rats. A slightly oversized hole, which did not pass through to the rear side of the bone, was created using a low-speed rotary drill. Subsequently, the implants were inserted into these holes, and then the subcutaneous tissue and skin were closed and sterilized.

The rats were sacrificed after a period of 14 d, and the implants with their surrounding tissue were retrieved. The specimens were fixed in a 10% neutral buffered formalin solution, dehydrated in a graded series of ethanol, and embedded in methylmethacrylate. Following polymerization, each implant block was sectioned into 20 μm thick slices. These sections were then stained with toluidine blue.

The sum of the linear bone contact with the implant surface was measured and was expressed as a percentage over the entire implant length (the bone-implant contact ratio, $R_{B\text{-}I}$) in the cancellous bone and the cortical bone parts. Significant differences in the bone-implant contact ratio were analyzed statistically using the Tukey–Kramer method.[27] Differences were considered statistically significant at the $p < 0.05$ level. This animal study was conducted in the laboratory of AAALAC International (Association for Assessment and Accreditation of Laboratory Animal Care International).

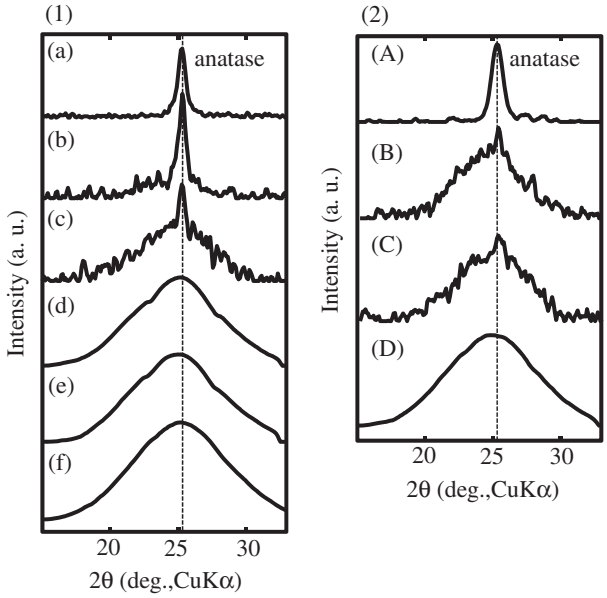

Fig. 1 XRD patterns of Ti (1) anodized up to 200 V in (a) 0.1 M, (b) 1 M, (c) 3 M, (d) 4 M, (e) 5 M, and (f) 9 M H_3PO_4 aqueous solution (298 K), and (2) anodized in 7.3 M H_3PO_4 aqueous solution (298 K) up to (A) 100 V, (B) 160 V, (C) 180 V, and (D) 200 V at a rate of 0.1 V s^{-1}.

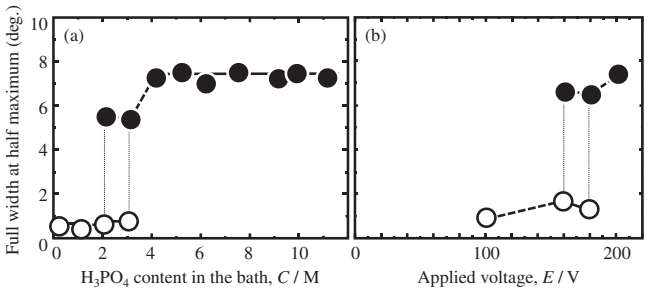

Fig. 2 Relationship between full width of half maximum of anatase peak in XRD pattern located at 2θ (deg) = 25.2 and (a) H_3PO_4 content in the bath anodized up to 200 V or (b) applied voltage in 7.3 M H_3PO_4 aqueous solution, classified with the crystal phase of TiO_2 (○: crystallized anatase and ●: amorphous anatase).

3. Results and Discussion

3.1 Surface properties of TiO_2 coatings

The XRD patterns of the anodized specimens are shown in Fig. 1, and the variations of full width at half maximum (FWHM) of the anatase peak, detected in the XRD pattern at 2θ (deg.) = 25.2, are shown in Figs. 2(a) and 2(b) as a function of H_3PO_4 content in the bath and applied voltage. In the same way as FWHM, variations in the PO_4^{3-} content in the oxide films, which were represented as the intensity ratio of P 2p/Ti 2p obtained in the XPS spectra, are shown in Fig. 3 as a function of H_3PO_4 content in the bath. Figure 4 shows the cross-sectional bright field image and ED image of the oxide film anodized up to 200 V in 9 M H_3PO_4. Figure 5 shows the surface SEM images of the substrate before and after anodizing.

The XRD patterns of the anodized specimens showed anatase peaks with different FWHM values. One was crystallized anatase with low FWHM values (<1 deg.)

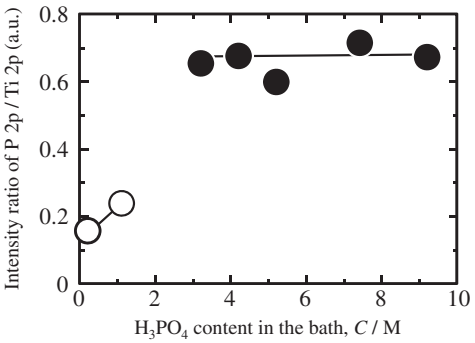

Fig. 3 Relationship between H_3PO_4 content in the bath and the amount of PO_4^{3-} contained in the coatings during anodizing up to 200 V at a rate of 0.1 V s^{-1} in H_3PO_4 aqueous solution (298 K) (○: crystallized anatase and ●: amorphous anatase).

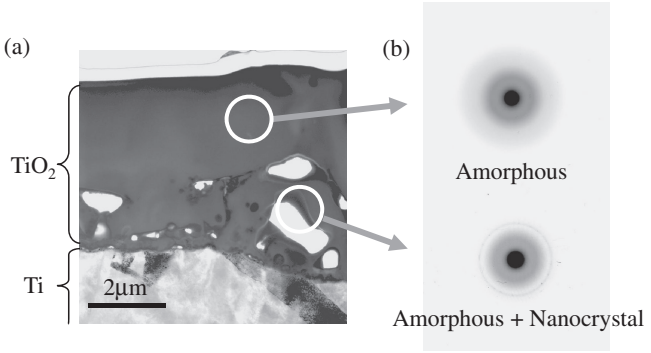

Fig. 4 (a) Cross-sectional bright field image by TEM and (b) ED patterns of Ti anodized in 9 M H_3PO_4 aqueous solution (298 K) up to 200 V at a rate of 0.1 V s^{-1}.

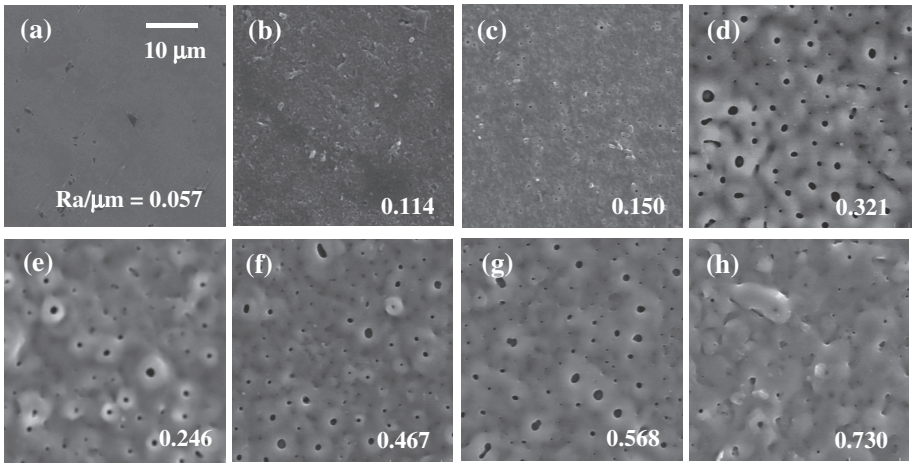

Fig. 5 Surface SEM images of (a) as-polished Ti, anodized Ti in (b) 0.1 M, (c) 1 M, (d) 3 M, (e) 4 M, (f) 5 M, (g) 7.3 M, and (h) 9 M H_3PO_4 aqueous solution up to 200 V at a rate of 0.1 V s^{-1}.

[Figs. 1(a) and 1(b)], and the other was an amorphous form with high FWHM values (>5 deg.) [Figs. 1(c), 1(d), and 1(e)]. The ED pattern meant that the oxide film consisted of anatase nanocrystals in the inner part and amorphous anatase on the nanocrystal phase.

When the FWHM values were arranged as a function of H_3PO_4 content in the bath (Fig. 2), it was found that the FWHM values suddenly increased from about 1 to 6 at 2 M, and maintained a constant high value of 8 above 4 M. This means that the amorphous structure can be obtained in H_3PO_4 aqueous solutions at concentrations higher than 2 M. Because sparking occurred during anodizing in these concentrated H_3PO_4 solutions, many pores were formed, which made the Ra value much higher than that of the original Ti surface [Figs. 5(d), 5(e), 5(f), 5(g), and 5(h)]. Crystallized TiO_2 films with low FWHM values were formed in H_3PO_4 solutions below 2 M. These films showed a relatively fine surface [Figs. 5(b) and 5(c)], similar to the original Ti substrate [Fig. 5(a)], because no sparking occurred during anodizing. These results mean that spark generation also influenced the crystallinity of the anatase films.

From XPS results, all of these anodized films were found to contain PO_4^{3-}, and its content depended on the concentration of H_3PO_4 in the bath (Fig. 3). In this figure, the data can be classified into two areas of high PO_4^{3-} content and low PO_4^{3-} content in the film at around 3 M. In each of the areas, PO_4^{3-} content in the film was almost constant irrespective of H_3PO_4 content in the bath. The same tendency was observed with the FWHM value. This implies that the FWHM value of the anatase peak corresponds to the PO_4^{3-} content in the oxide film. In other words, the formation of the amorphous phase seemed to be caused by incorporation of PO_4^{3-} into the crystal lattice. Therefore, a large amount of PO_4^{3-} in the lattice was considered to disturb the formation of the ordered crystal structure of TiO_2, resulting in the formation of the amorphous phase. Saturation of PO_4^{3-} in the crystal lattice seems to be responsible for the constant FWHM value above 4 M.

However, the concentration of H_3PO_4 was not the only factor in forming the amorphous phase. Despite sufficient PO_4^{3-} in 7.3 M H_3PO_4 solutions, the amorphous phase was not observed at low voltages that did not generate sparking [Fig. 1(2)(A)]. Thus, sparking seemed to work as a trigger to incorporate PO_4^{3-} into the film. Therefore, the amorphous phase could be caused by spark generation during anodizing in concentrated H_3PO_4 solution. To summarize the crystallinity of the anatase film in relation to H_3PO_4 content in the bath and applied voltage, it was classified into two groups,

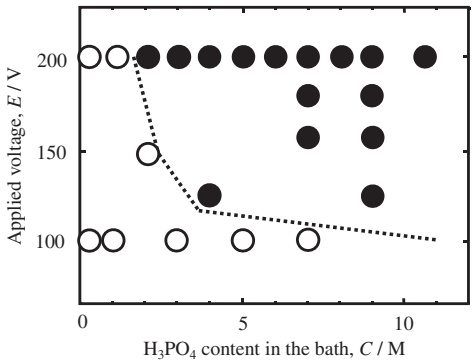

Fig. 6 Classified crystal phase of TiO_2 in relation to H_3PO_4 content in the bath and applied voltage (○: crystallized anatase and ●: amorphous anatase).

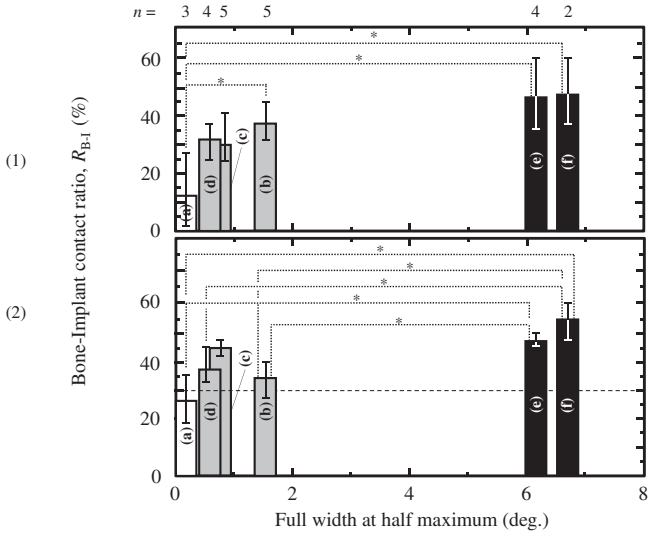

Fig. 7 Bone-implant contact ratio, $R_{B\text{-}I}$ of the specimens (a) as-polished, anodized up to 100 V in (b) 0.1 M H_3PO_4, and up to 200 V in (c) 0.1 M H_3PO_4 solution, (d) 1 M H_3PO_4 solution, (e) 5 M H_3PO_4, and (f) 9 M H_3PO_4 solution when implanted in (1) cortical bone part and (2) cancellous bone part: $^*p < 0.05$.

as shown in Fig. 6. This figure also shows that the amorphous phase could be obtained by an increase in both H_3PO_4 content in the bath and applied voltage.

3.2 *In vivo* evaluation

Because of the good correlation between the FWHM value and PO_4^{3-} content in the films, as noted above, the following descriptions are discussed in terms of the FWHM values. Figure 7 shows the bone-implant contact ratios, $R_{B\text{-}I}$, of specimens in both the cortical bone part and the cancellous bone part. As this figure illustrates, all of the anodized specimens showed higher $R_{B\text{-}I}$ values [(b)–(f)] than as-polished [(a)]. Focusing on the specimens with anatase films, specimens with high FWHM values (black bars, anodized in 5 M and 9 M H_3PO_4) tended to have higher $R_{B\text{-}I}$ values in both the cortical and the cancellous bone parts than specimens with low FWHM values in the film (gray bars, anodized in 0.1 M and 1 M H_3PO_4). In general, the bone-forming ability of implants is said to be influenced by film properties such as surface roughness,[26] crystal structure,[21,24] and the type of electrolyte ions.[28] However, the crystal structure and the type of electrolyte ions did not show a relation to the difference in $R_{B\text{-}I}$ values among anodized specimens because all of the anodized films had the same crystal structure (anatase) and contained the same anion (PO_4^{3-}) in the films. On the other hand, surface roughness, the crystallinity of anatase, and/or PO_4^{3-} content in the film might have influence on the osteoconductivity because each of the anodized specimens had different Ra, FWHM values, and PO_4^{3-} content in the film. As for the influence of surface roughness on the $R_{B\text{-}I}$ value, anodized specimens with a rough surface ($0.467 \leq Ra/\mu m \leq 0.730$) showed higher $R_{B\text{-}I}$ values than anodized specimens with a fine surface ($0.082 \leq Ra/\mu m \leq 0.150$). This result does not agree with our previous report saying that a rough surface ($Ra/\mu m > 0.3$) was not better for hard tissue formation than a fine surface ($Ra/\mu m < 0.3$).[26] On the other hand, the $R_{B\text{-}I}$ values of anatase changed corresponding to the FWHM values and PO_4^{3-} content in the film, and amorphous anatase coatings tended to show higher $R_{B\text{-}I}$ values than crystallized anatase coatings. This means that incorporation of PO_4^{3-} in the film improves the osteoconductivity of anatase, and that the crystallinity of anatase and/or PO_4^{3-} content in the film had stronger influence on the $R_{B\text{-}I}$ values of anatase films than surface roughness. However, it was not clear which of crystallinity of anatase or PO_4^{3-} content in the film was intrinsic factor to influence the osteoconductivity of amorphous anatase because of interdependency of them. The scarcity of *in vivo* reports on the influence of crystallinity and PO_4^{3-} content in the film on bone formation also makes it difficult to discuss the relative importance of the two factors. We will discuss the relationship between crystallinity and osteoconductivity in more detail in a future report, using TiO_2 films whose crystallinity is controlled by another hydro-processing.

4. Conclusions

In this study, the effects of H_3PO_4 content in the bath and applied voltage on the crystal structure of TiO_2 films were investigated, and the following findings were obtained.

(1) Anatase coating was formed on Ti using anodizing regardless of the concentration of H_3PO_4. Particularly when Ti substrates were anodized under spark discharge in concentrated H_3PO_4 aqueous solutions, the amorphous phase was formed in addition to the crystallized phase. The amorphous phase was formed by incorporating a large amount of PO_4^{3-} into the TiO_2 crystal lattice.

(2) The amorphous anatase films showed a larger amount of hard tissue formation on their surface than crystallized anatase films in both of the cortical bone part and cancellous bone part. This means that incorporation of PO_4^{3-} in anatase film improves the osteoconductivity of anatase.

(3) It is not exactly clear what was the dominant factor to influence the osteoconductivity of anatase, but the crystallinity of anatase and/or PO_4^{3-} in the film are considered to be the reason to make the difference in bone-forming ability of TiO_2 films.

Acknowledgements

This work was partially supported by a Grant-in-Aid for Scientific Research (C) (No. 21560719), Grant-in-Aid for JSPS fellows (No. 2310401), and the Global COE program (COE for Education and Research of Micro-Nano Mechatronics) from the Japan Society for the Promotion of Science (JSPS).

REFERENCES

1) R. Adell, B. Eriksson, U. Lekholm, P. I. Branemark and T. Jemt: Int. J. Oral Maxillofac. Implants **5** (1990) 347–359.
2) D. van Steenberghe, U. Lekholm, C. Bolender, T. Folmer, P. Henry, I. Herrmann, K. Higuchi, W. Laney, U. Linden and P. Astrand: Int. J. Oral Maxillofac. Implants **5** (1990) 272–281.
3) R. A. Jaffin and C. L. Berman: J. Periodontol. **62** (1991) 2–4.
4) W. Khang, S. Feldman, C. E. Hawley and J. Gunsolley: J. Periodontol. **72** (2001) 1384–1390.
5) K. Kuroda, R. Ichino, M. Okido and O. Takai: J. Biomed. Mater. Res. **59** (2002) 390–397.
6) K. Kuroda, R. Ichino, M. Okido and O. Takai: J. Biomed. Mater. Res. **61** (2002) 354–359.
7) K. Kuroda, Y. Miyashita, R. Ichino, M. Okido and O. Takai: Mater. Trans. **43** (2002) 3015–3019.
8) K. Kuroda, S. Nakamoto, R. Ichino, M. Okido and R. M. Pilliar: Mater. Trans. **46** (2005) 1633–1635.
9) K. Kuroda, S. Nakamoto, Y. Miyashita, R. Ichino and M. Okido: Mater. Trans. **47** (2006) 1391–1394.
10) K. Kuroda, M. Moriyama, R. Ichino, M. Okido and A. Seki: Mater. Trans. **49** (2008) 1434–1440.
11) K. Kuroda, M. Moriyama, R. Ichino, M. Okido and A. Seki: Mater. Trans. **50** (2009) 1190–1195.
12) R. Hazan, R. Brener and U. Oron: Biomaterials **14** (1993) 570–574.
13) S. Fujibayashi, M. Neo, H.-M. Kim, T. Kokubo and T. Nakamura: Biomaterials **25** (2004) 443–450.
14) L. Jonasova, F. A. Muller, A. Helebrant, J. Strnad and P. Greil: Biomaterials **25** (2004) 1187–1194.
15) F. Xiao, K. Tsuru, S. Hayakawa and A. Osaka: Thin Solid Films **441** (2003) 271–276.
16) J.-M. Wu, S. Hayakawa, K. Tsuru and A. Osaka: Scr. Mater. **46** (2002) 101–106.
17) K.-R. Wu, C.-H. Ting, W.-C. Lie, C.-H. Lin and J.-K. Wu: Thin Solid Films **500** (2006) 110–116.
18) L. S. Hsu, R. Rujkorakarn, J. R. Sites and C. Y. She: J. Appl. Phys. **59** (1986) 3475–3480.
19) Y.-T. Sul, C. B. Johansson, S. Petronis, A. Krozer, Y. S. Jeong, A. Wennerberg and T. Albreksson: Biomaterials **23** (2002) 491–501.
20) J. P. Schreckenbach, G. Marx, F. Schlotigg, M. Textor and N. D. Spencer: J. Mater. Sci. Mater. Med. **10** (1999) 453–457.
21) B. Yang, M. Uchida, H.-M. Kim, X. Zhang and T. Kokubo: Biomaterials **25** (2004) 1003–1010.
22) L. A. de Sena, N. C. C. Rocha, M. C. Andrade and G. A. Soares: Surf. Coat. Tech. **166** (2003) 254–258.
23) N. K. Kuromoto, R. A. Simao and G. A. Soares: Mater. Charact. **58** (2007) 114–121.
24) X. Cui, H.-M. Kim, M. Kawashita, L. Wang, T. Xiong, T. Kokubo and T. Nakamura: Dent. Mater. **25** (2009) 80–86.
25) J.-H. Lee, S.-E. Kim, Y.-J. Kim, C.-S. Chi and H.-J. Oh: Mater. Chem. Phys. **98** (2006) 39–43.
26) D. Yamamoto, I. Kawai, K. Kuroda, R. Ichino, M. Okido and A. Seki: Mater. Trans. **52** (2011) 1650–1654.
27) C. Y. Kramer: Biometrics **12** (1956) 307–310.
28) D. Wei, Y. Zhou, D. Jia and Y. Wang: Surf. Coat. Tech. **201** (2007) 8723–8729.